Applied Numerical Modeling in Geomechanics – 2020 – Billaux, Hazzard, Nelson & Schöpfer (eds.) Paper: 16-05

FLAC3D modeling of geocell reinforced foundation beds

Amarnath Hegde & Hasthi Venkateswarlu
Department of Civil and Environmental Engineering, Indian Institute of Technology Patna, India

1 INTRODUCTION

Over the years, geosynthetic reinforcements have been used in various civil engineering applications. These materials are available in different shapes and forms to suit specific applications. Geosynthetics have replaced the use of conventional reinforcement materials like metallic products and steel bars. Among the different forms, geocells are relatively new and known for offering economical, efficient, and environmentally friendly solutions. Several studies reported the potential benefits of using geocells in the field of geotechnical engineering through field and laboratory studies (Hegde 2017).

On the other hand, numerical simulation of geocell is considered to be complex due to its honeycomb structure. A very few studies have successfully demonstrated the numerical simulation of geocell (Hegde & Sitharam 2015a, b). Over the years, the numerical modeling of geocell reinforced beds has slowly evolved. The ECA (Equivalent Composite Approach) was among the first few approaches of modeling geocell in a two-dimensional framework. Due to its simplicity, various researchers have adopted it to model the geocells (Hegde & Sitharam 2013). In ECA, infill material and the geocell are modeled as a composite soil layer with enriched stiffness and strength properties. Bathurst & Karpurapu (1993) and Rajagopal et al. (1999) provided suitable formulae to quantify the properties of the equivalent composite layer. Later, some of the researchers modeled the geocell with square, circular and hexagonal shaped pockets (Hegde 2017). Hegde & Sitharam (2015c) successfully demonstrated the modeling of actual honeycomb shape of the geocells using three-dimensional finite difference package *FLAC3D* (Itasca 2012). The study highlighted that the modeling of geocell as per square geometry results in the non-uniform distribution of the stresses in geocells. In the present study, the methodology proposed by Hegde & Sitharam (2015c) has been used to investigate the static and dynamic response of geocell reinforced foundation beds. In the modeling, the multiple geocell pockets were modeled according to the actual curvature of the individual cells. The explicit finite difference package *FLAC3D* was chosen to develop the models due to its efficacy in solving static and time domain problems. Further, Hegde et al. (2016) recommended to use *FLAC3D* over PLAXIS3D for simulations of geocells due to the availability of robust structural elements in the former. In the present study, to validate the developed *FLAC3D* models, results of static plate load tests reported by Hegde & Sitharam (2015a) were used. Similarly, results of field vibration tests reported by Venkateswarlu et al. (2018) was used for the dynamic case.

2 MODELING METHODOLOGY

2.1 *Modeling of geocell reinforced beds under static loading conditions*

Hegde & Sitharam (2015a) performed static plate load tests on the geocell reinforced sand bed in a test tank having the dimensions of 900 mm × 900 mm × 600 mm. A square steel plate of 150 mm size and 20 mm thickness was used as a footing. The manually operated hydraulic jack connected with the loading frame was used for applying the load. The poorly graded sand (SP) was used for the preparation of test bed and

filling the geocell pockets. The experimental condition was simulated using *FLAC3D* to study the pressure distribution pattern. Only the quarter portion of the soil bed was considered for developing the numerical model due to the symmetry. The Mohr Coulomb model was used to simulate the constitutive behavior of the infill and foundation soil. The geogrid structural element was used to model the actual geometry of geocell. To do that, coordinates of the actual curvature of pockets were acquired from the photograph of the expanded geocell through the digitization process. The obtained coordinates were used to model the 3D honeycomb shape of the geocell as shown in Fig. 1a. The behavior of the geocell was simulated using the linear elastic model. The interfaces between the geocell and the soil were also modeled using Mohr Coulomb yield criterion. The analyses were performed under the controlled velocity loading of 2.5 × E–5 m/step. The various properties of the sand, geocell, and interface behavior between the sand and geocell used in the modeling are listed in Table 1.

Table 1. Properties of various materials used in modeling under static loading condition.

Material	Parameters	Values
Sand	Shear modulus, G (MPa)	5.77
	Bulk modulus, K (MPa)	12.5
	Poisson's ratio	0.3
	Cohesion, C (kPa)	0
	Friction angle, φ (º)	36
	Unit weight, γ_d (kN/m^3)	20
Geocell	Young's modulus, E (MPa)	275
	Poisson's ratio, v	0.45
	Interface shear modulus, ki (MPa/m)	2.36
	Interface cohesion, ci (kPa)	0
	Interface friction angle, φ_i (°)	30
	Thickness, t_i (mm)	1.5

All the listed parameters were determined through various laboratory tests as suggested by Hegde & Sitharam (2015a). To model the actual test conditions, the displacement along the bottom face of the model was fixed in both the horizontal and vertical directions. The vertical faces of the model were fixed in the horizontal direction to allow displacement in the vertical direction.

2.2 *Modeling of geocell reinforced beds under vertical mode dynamic excitation*

Venkateswarlu et al. (2018) performed a series of field vibration tests on the unreinforced and geocell reinforced foundation beds to understand the dynamic response. The numerical simulation of the experimental setup was performed in *FLAC3D* to understand the dissipation mechanism of the vibration. As an initial step of the simulation, the subsurface profile of the test site was modeled up to the depth of 10 m (as shown in Fig. 2a). The brick element was used for this purpose. The unreinforced and geocell reinforced foundation beds of size 2 m × 2 m × 1.2 m were simulated at the existing ground surface. The concrete block was simulated over the foundation bed and the static stress was applied. The magnitude of static stress was equal to the stresses caused by the machine parts and self-weight of footing. In the second step, the vertical mode dynamic excitation was applied over the block by considering the time interval of 10 sec. The *FISH* programming code was used for simulating the dynamic excitation over the concrete block to replicate the vibration induced from the machines. The frequency of the dynamic excitation was varied from 0 to 45 Hz during the analysis. In the final step, dynamic excitation was turned off and the soil was allowed to vibrate freely. The properties of the various materials used in the development of a numerical model are summarized in Table 2. In the dynamic analysis, Mohr Coulomb and linear elastic constitutive models were used to simulate the behavior of infill material and geocell reinforcement, respectively. The geocell was placed at the depth of 0.1B (B is the width of the footing) under the footing. In order to simulate the far field response of the site, quiet boundaries were applied to the extreme (vertical and horizontal) boundaries of the numerical model. It helps in minimizing the wave reflections into the system from the

model boundaries. In order to simulate the vibration decay in the soil system, 5% material damping was considered for all the soil layers (Ujjawal et al. 2019). The Poisson's ratio of all the soil layers was considered as 0.3 in the numerical analysis (Venkateswarlu & Hegde 2018).

Table 2. Properties of different materials used in modeling for dynamic loading condition.

Material	Parameter	Value
Foundation soil (Silty sand)	Unit weight, γ_d (kN/m^3)	17.45
	Angle of shearing resistance, φ (º)	32
	Cohesion, C (kPa)	2
	Young's modulus, E (MPa)	20
Subsurface details 0 m - 1.1 m (Silty clay)	Young's modulus, E (MPa)	5.1
	Cohesion, C (kPa)	48
	Angle of shearing resistance, φ (º)	3
	Dynamic elastic modulus, (MPa)	38.2
	Unit weight, γ_d (kN/m^3)	16.3
1.1 m – 3.35 m (Loose sand)	Young's modulus, E (MPa)	25.2
	Cohesion, C (kPa)	1
	Angle of shearing resistance, φ (º)	30
	Dynamic elastic modulus, (MPa)	151
	Unit weight, γ_d (kN/m^3)	17.8
3.35 m – 10 m (Dense sand)	Young's modulus, E (MPa)	51
	Cohesion, C (kPa)	1
	Angle of shearing resistance, φ (º)	36
	Dynamic elastic modulus, (MPa)	256
	Unit weight, γ_d (kN/m^3)	18.4
Concrete footing	Elastic modulus of concrete, E_c (MPa)	2×10^4
	Unit weight of concrete, γ_c (kN/m^3)	24
	Poisson's ratio of concrete, v_c	0.15
Geocell	Young's modulus, E (MPa)	275
	Poisson's ratio, v	0.45
	Thickness, t_i (mm)	1.53
	Interface shear modulus, k_i (MPa/m)	2.36
	Interface cohesion, c_i (kPa)	0
	Interface friction angle, φ_i (º)	30

3 RESULTS AND DISCUSSION

The static response of unreinforced and geocell reinforced foundation beds obtained from numerical study was found to be in good agreement with the experimental results as shown in Figure 1b. The stress distribution contours of both unreinforced and geocell reinforced cases corresponding to the vertical stress of 200 kPa are shown in Figure 1c-d. In the case of unreinforced bed, the uniform stress distribution was noticed up to the greater depth under the footing. Whereas, the stresses are transmitted to a shallow depth in the presence of geocell reinforcement. Geocells found to distribute the load to wider areas in the lateral direction. Further, the stress contours indicated that the observed results were not influenced by the tank boundaries.

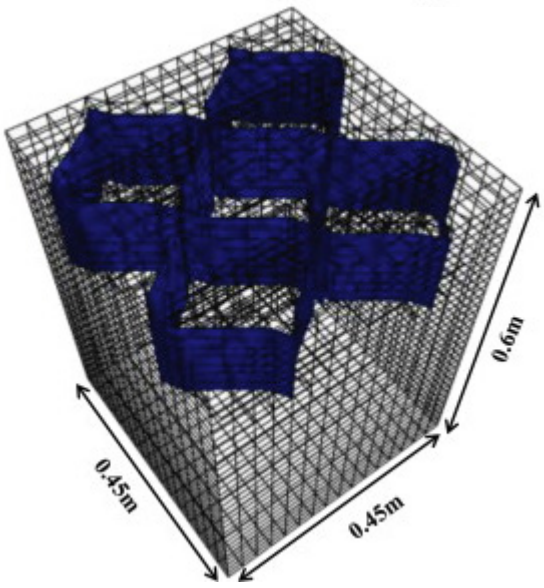

(a) *FLAC3D* model for geocell reinforced case

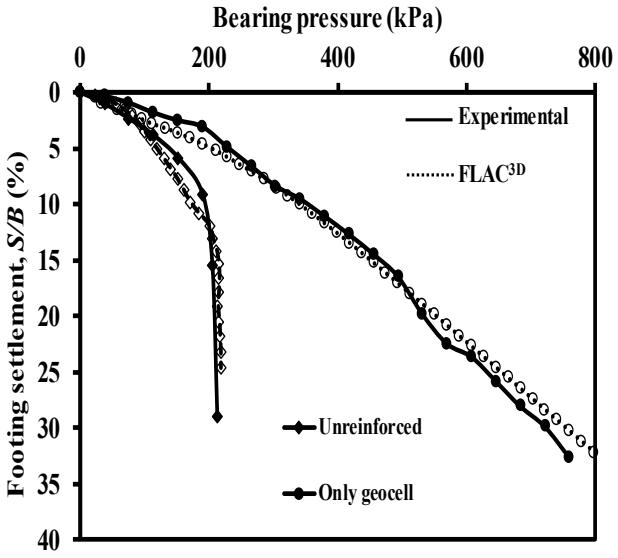

(b) Experimental versus numerical comparison

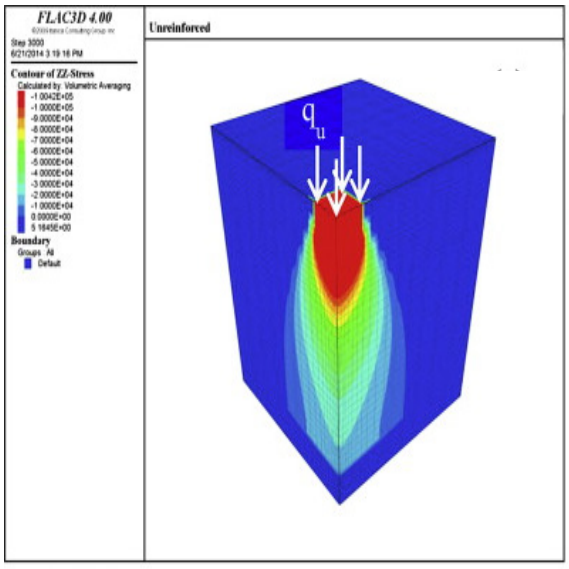

(c) Stress distribution of unreinforced case

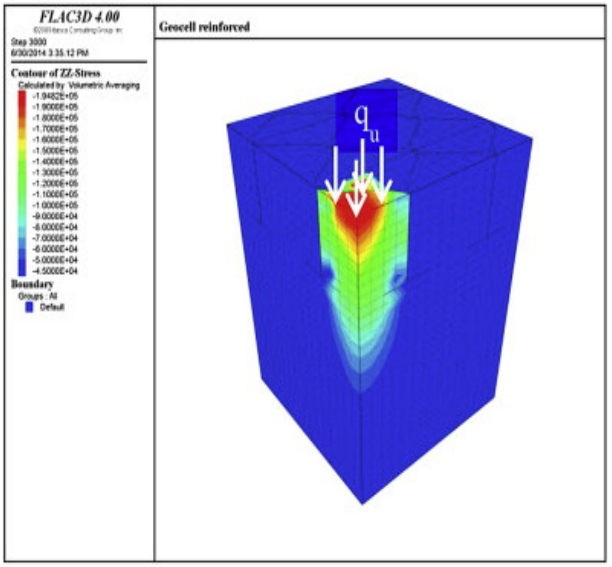

(d) Stress distribution of geocell reinforced case

Figure 1. Static response of unreinforced and geocell reinforced cases (modified after Hegde & Sitharam 2015a).

Figure 2a-d shows the *FLAC3D* model, validation and results of the geocell reinforced foundation beds subjected to dynamic loading. The numerical displacement amplitude versus frequency response of unreinforced and geocell reinforced cases has shown good agreement with the experimental results (Fig. 2b). The lateral spreading of vibration was extended up to 6*B* (*B* is the width of footing) in the case of unreinforced condition (Fig. 2c). Whereas, it was restricted to 3*B* in the presence of geocell (Fig. 2d). The displacement contours corresponding to frequency of 30 Hz are reported in the figure. Geocells enhances the radiation damping of the foundation bed to confine the lateral spreading of the vibration.

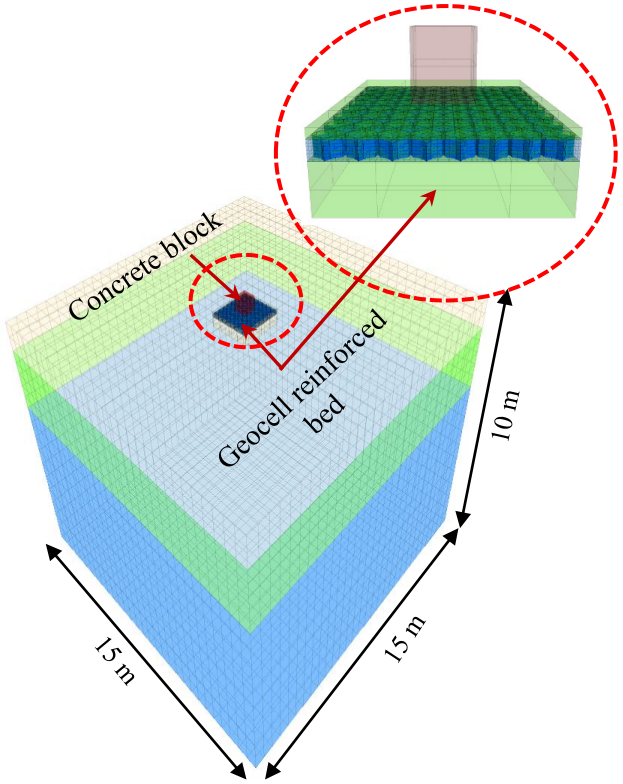

(a) Finite difference model

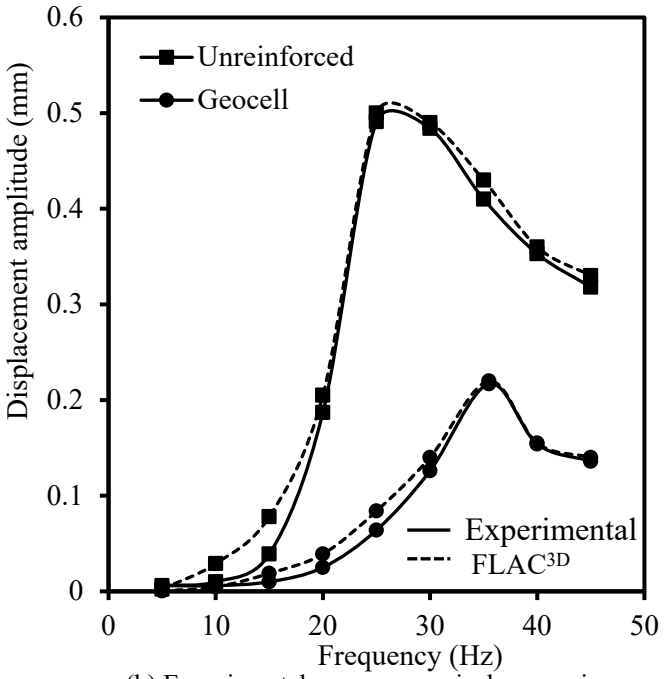

(b) Experimental versus numerical comparison

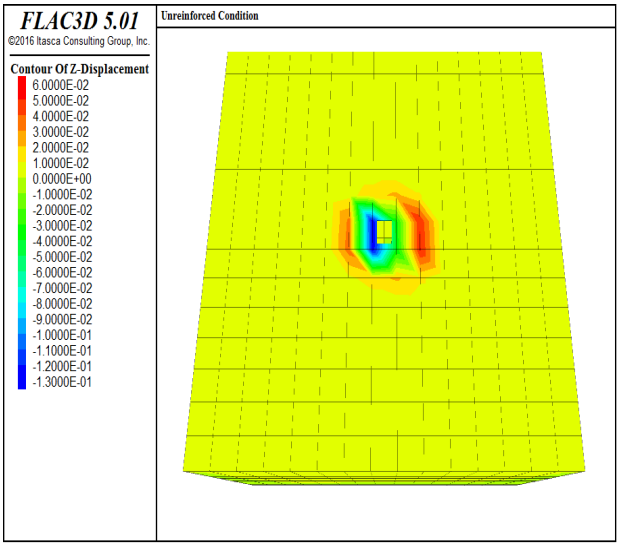

(c) Lateral spreading of vibration in unreinforced case

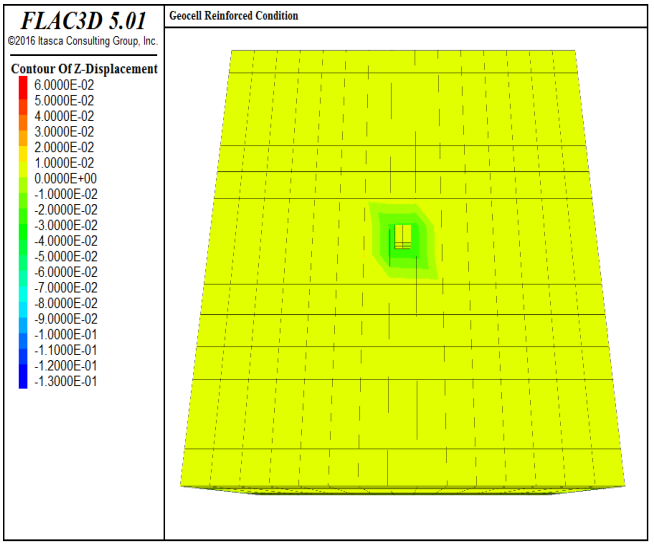

(d) Lateral spreading of vibration in geocell reinforced case

Figure 2. Dynamic response of unreinforced and geocell reinforced cases (modified after Venkateswarlu et al. 2018).

4 CONCLUSIONS

FLAC3D numerical simulations were successfully used for predicting the static and dynamic response of geocell reinforced beds. Encouraging agreement was observed between the numerical and experimental results in both the cases. In case of the static loading, geocell found to distribute the load in the lateral

direction to wider areas. In case of the dynamic loading, geocell found to confine the lateral spreading of induced vibration. In overall, *FLAC3D* was found robust in analyzing the static and dynamic problems involving geocells.

REFERENCES

Bathurst, R. J. & Karpurapu, R. 1993. Large-scale triaxial compression testing of geocell-reinforced granular soils. *Geotechnical Testing Journal*, 16(3), 296-303.

Hegde, A. 2017. Geocell reinforced foundation beds-past findings, present trends and future prospects: A state-of-the-art review. *Construction and Building Materials*, 154, 658-674.

Hegde, A. & Sitharam, T.G. 2015a. 3-dimensional numerical modelling of geocell reinforced sand beds. *Geotextiles and Geomembranes*, 43, 171-181.

Hegde, A. M. & Sitharam, T. G. 2015b. Experimental and numerical studies on protection of buried pipelines and underground utilities using geocells. *Geotextiles and Geomembranes*, 43(5), 372-381.

Hegde, A.M. & Sitharam, T.G. 2015c. Three-Dimensional numerical analysis of geocell reinforced soft clay beds by considering the actual geometry of geocell pockets. *Canadian Geotechnical Journal*, 52, 1-12.

Hegde, A. & Sitharam, T. G. 2013. Experimental and numerical studies on footings supported on geocell reinforced sand and clay beds. *International Journal of Geotechnical Engineering*, 7(4), 346-354.

Hegde. A. Shivdev. S. & Sitharam, T.G. 2016. Numerical Simulation of Geocell Reinforced Foundation Beds: A Comparative Study Using PLAXIS3D and *FLAC3D*. *Proceedings of Indian Geotechnical Conference*-2016, 15-17 December, Chennai, Paper ID 365 (CD-ROM).

Itasca Consulting Group, Inc. 2012. *FLAC3D – Fast Lagrangian Analysis of Continua in 3 Dimensions, Ver. 5.0*. Minneapolis: Itasca.

Rajagopal, K. Krishnaswamy, N. R. & Latha, G. M. 1999. Behaviour of sand confined with single and multiple geo-cells. *Geotextiles and Geomembranes*, 17(3), 171-184.

Ujjawal, K. N. Venkateswarlu, H. & Hegde, A. 2019. Vibration isolation using 3D cellular confinement system: A numerical investigation. *Soil Dynamics and Earthquake Engineering*, 119, 220-234.

Venkateswarlu, H. & Hegde, A. 2018. Numerical Analysis of Machine Foundation Resting on the Geocell Reinforced Soil Beds. *Geotechnical Engineering*, 49(4), 55-62.

Venkateswarlu, H. Ujjawal, K. N. & Hegde, A. 2018. Laboratory and numerical investigation of machine foundations reinforced with geogrids and geocells. *Geotextiles and Geomembranes*, 46(6), 882-896.